**Atmospheric
Chemistry
and Physics
Discussions**

Cloud phase from
POLDER and MODIS
data

J. Riedi et al.

Cloud thermodynamic phase inferred from merged POLDER and MODIS data

J. Riedi[1]**, B. Marchant**[1]**, S. Platnick**[2]**, B. Baum**[3]**, F. Thieuleux**[1]**, C. Oudard**[1]**,
F. Parol**[1]**, J-M. Nicolas**[4]**, and P. Dubuisson**[1]

[1]Laboratoire d'Optique Atmosphérique, Université des Sciences et Technologies de Lille,
France
[2]NASA Goddard Space Flight Center, MD, USA
[3]SSEC, University of Wisconsin-Madison, WI, USA
[4]ICARE Data and Services Center, Université des Sciences et Technologies de Lille, France

Correspondence to: J. Riedi, jerome.riedi@univ-lille1.fr

Title Page

Abstract	Introduction
Conclusions	References
Tables	Figures

◄◄	►►
◄	►
Back	Close

Full Screen / Esc

Printer-friendly Version

Interactive Discussion

EGU

Full Screen / Esc

Printer-friendly Version

Interactive Discussion

EGU

Abstract

The global spatial and diurnal distribution of cloud properties is a key issue for understanding the hydrological cycle, and critical for advancing efforts to improve numerical weather models and general circulation models. Satellite data provides the best way of gaining insight into global cloud properties. In particular, the determination of cloud thermodynamic phase is a critical first step in the process of inferring cloud optical and microphysical properties from satellite measurements. It is important that cloud phase be derived together with an estimate of the confidence of this determination, so that this information can be included with subsequent retrievals (optical thickness, effective particle radius, and ice/liquid water content).

In this study, we combine three different and well documented approaches for inferring cloud phase into a single algorithm. The algorithm is applied to data obtained by the MODIS (MODerate resolution Imaging Spectroradiometer) and POLDER3 (Polarization and Directionality of the Earth Reflectance) instruments. It is shown that this synergistic algorithm can be used routinely to derive cloud phase along with an index that helps to discriminate ambiguous phase from confident phase cases.

The resulting product provides a semi-continuous confidence index ranging from confident liquid to confident ice instead of the usual discrete classification of liquid phase, ice phase, mixed phase (potential combination of ice and liquid particles), or simply unknown phase clouds. This approach is expected to be useful for cloud assimilation and modeling efforts while providing more insight into the global cloud properties derived from satellite data.

1 Introduction

Clouds are important modulators of the Earth's radiation budget and hydrological cycle. Their macrophysical, microphysical, and optical properties (cloud pressure, temperature, height, optical thickness, thermodynamic phase, effective particle size) and their

variation in space and time need to be understood to improve general circulation and weather prediction models. Additionally, cloud properties are being used increasingly in nowcasting activities as part of data assimilation efforts. For nowcasting, the cloud thermodynamic phase is an important indicator used by forecasters to determine hazardous road conditions.

The determination of cloud thermodynamic phase is critical for inferring optical thickness and particle size because ice and water clouds have very different scattering and absorption properties. The quality of the retrieval depends on the ability to match pre-computed radiative transfer calculations with measurements. It is thus critical that cloud phase be derived together with an estimate of its confidence to help decide which optical models should be used for determination of optical thickness, effective particle radius and ice/liquid water content.

Recent efforts have been made to derive cloud thermodynamic phase from satellite-based passive radiometric observations (e.g., Knap et al., 2002; Baum et al., 2000; Key and Intrieri, 2000; Goloub et al., 2000; Platnick et al., 2003) but no single method is expected to be preferable for all cloud types and regions. Atmospheric or surface properties can bias existing methods or lead to ambiguous results. Further, a single unambiguous answer is inappropriate for multilayer cloud systems (Baum et al., 2003; Pavolonis and Heidinger, 2004) or mixed phase clouds (Pavolonis et al., 2005). Yet, both cases are recognized as significant components of the global cloud cover (Hahn et al., 1982; Hahn et al., 1984). There is a great interest for new approaches that can provide more meaningful cloud thermodynamic phase information from passive imagers on a global scale.

The approach proposed in this study is based on the synergy between the POLDER-3/Parasol (POLarization and Directionality of the Earth Reflectances) and MODIS/Aqua (MODerate resolution Imaging Spectroradiometer) instruments operating in the framework of the A-Train mission. Both POLDER and MODIS have been used to derive key parameters needed to improve our knowledge of cloud

properties (Platnick et al., 2003; Parol et al., 2004).

The potential of using polarization measurements of the reflected shortwave radiation to infer cloud phase has been clearly demonstrated using POLDER observations (Goloub et al., 2000; Riedi et al., 2001). The MODIS instrument provides information on cloud phase using two methods that rely on spectral measurements in the visible, shortwave to midrange infrared, and thermal infrared Platnick et al. (2003). However, both the instruments and the specifically designed retrieval algorithms have limitations that need to be understood and recognized to prevent drawing misleading conclusions from analysis of the data products. Fortunately, limitations from one instrument can partly be mitigated by capabilities available from the other, as will be demonstrated in this paper.

We present a methodology to combine these three different and well documented approaches for deriving cloud phase within a single algorithm that uses data from both the MODIS and POLDER instruments. A brief description of the processing algorithm used to merge radiance data from MODIS and POLDER is provided in Sect. 3.

POLDER level 1b (L1B) data files correspond to a complete daytime portion of an orbit (equivalent to approximately 40 min of data acquisition). For each POLDER L1B file, the corresponding MODIS data (radiances and geolocation) are collocated with POLDER data on a common sinusoidal grid centered on the POLDER ascending node longitude. For each element within that grid ($6 \times 6 \, km^2$) observed by both instruments, we form a data structure that contains all multidirectional and multispectral POLDER data together with all multispectral and multiresolution MODIS data. For MODIS, within each element of the grid, the mean and standard deviation for each radiance is computed and kept along with all individual full resolution data (250 m, 500 m and 1 km). These L1B radiances are provided together with surface albedo information derived from MODIS (Moody et al., 2005) and meteorological data (obtained for the European Center for Medium-Range Weather Forecast) needed for retrieval of cloud properties.

Cloud phase from POLDER and MODIS data

J. Riedi et al.

Title Page

Abstract	Introduction
Conclusions	References
Tables	Figures

◀◀ ▶▶

◀ ▶

Back Close

Full Screen / Esc

Printer-friendly Version

Interactive Discussion

EGU

In the first part of the paper, we provide an overview of the theoretical basis of the three methods for cloud phase discrimination with particular emphasis on their respective strengths and limitations. In the second part, the processing scheme for the joint MODIS/POLDER data analysis is briefly discussed and the practical implementation of the joint algorithm described. A case study, featuring typhoon Nabi on September 2005 (Fig. 1), is then analyzed to show how this synergistic algorithm can be used routinely to derive a cloud phase index, along with information on retrieval quality/confidence usefull for easily discriminating ambiguous from confident cases.

The resulting product is provided as a semi-continuous index ranging from confident liquid only to confident ice only instead of the usual liquid/ice/mixed discrete phase classification. This approach is a necessary step towards being able to assess errors inherent in derived regional and global cloud products.

2 Theoretical basis overview

Figure 2 provides an overview of the three metrics used for phase discrimination in this study. The interpretation of these metrics will be discussed. For a case study to illustrate the theoretical basis for the three different methods, we have selected a region covered by Typhoon Nabi.

2.1 Multiangle polarization measurements

When considering a cloudy system observed from a satellite, the polarized component of the upwelling radiance is primarily from the upper portion of the cloud layer. Calculations have shown that the polarized component, Lp, is saturated for cloud optical thickness greater than 2–3 depending on the cloud microphysics that is represented by the particle shape and effective size. The important quantity for determining cloud

EGU

phase is the polarized radiance Lp, which is less sensitive than the total radiance[1] L to multiple scattering effects. Thus, the polarization features, which correspond to single scattering, are preserved in Lp.

According to both theory and observations (Chepfer et al., 2001; Bréon and Goloub, 1998; Goloub et al., 2000), the polarization features of clouds depend strongly on the particle shape and size. Within the range of scattering angles that can be observed by POLDER, clouds composed of liquid spherical particles exhibit a strong maximum in Lp at about 140°(primary rainbow). Liquid clouds exhibit a polarization value of zero (i.e., a neutral point) at around 90°, and supernumerary bows for angles greater than 145°. These features make possible the discrimination with clouds composed of ice particles, which exhibit positive polarization that decreases as the scattering angle increases (Fig. 2d). Unambiguous discrimination between ice particles and liquid water droplets can be made using these polarization differences.

Because it relies on the different single scattering properties of spherical and non-spherical particles, this cloud phase detection may be considered a cloud particle shape detection method. Ice clouds are typically composed of nonspherical particles, whereas liquid water clouds are assumed to be composed of spherical droplets. Also, the use of polarization measurements makes this technique primarily sensitive to the very top of the uppermost cloud layer since Lp saturates for cloud optical thickness greater than 2.

Finally, the use of polarized angular signatures depends on the availability of particular scattering angles, which means phase information will depend on the total number of viewing geometries and the the range of scattering angles available. An advantage of this technique is that it is insensitive to particle size and also to potential biases in inferred cloud temperature. A complete description of the operational implementation for this algorithm is given by Riedi et al., 2007[2].

---

[1]Also, the polarization degree, defined as the ratio of Lp over L, is subject to multiple scattering effects since it depends on L.

[2]Riedi, J., Parol, F., and Goloub, P.: Cloud Thermodynamic phase determination from multi-

EGU

2.2 Shortwave infrared and visible measurements

Pilewskie and Twomey (1987) recognized that reflectance measurements near 1.6 and 2.1 μm can provide useful information for cloud phase discrimination. For wavelengths in the shortwave infrared spectrum, the imaginary part of the refractive index becomes non-negligible for both water and ice, thereby causing absorption by cloud particles to occur at these wavelengths. For the MODIS 1.6 and 2.1 μm bands, the imaginary part is also greater for ice than for liquid water. With all other properties being equal, an ice cloud will exhibit higher absorption than a liquid cloud.

Since almost no absorption occurs at visible wavelengths, the ratio of shortwave infrared (SWIR) to visible (VIS) reflectances will be lower for an ice cloud than for a liquid cloud, assuming everything but phase is kept the same. Because ice particles are generally larger than liquid cloud droplets, we can derive cloud phase by simply applying threshold tests on the SWIR to VIS ratio. This will work as long as (i) the liquid cloud droplet size does not increase too much (or ice particles become very small), (ii) the optical thickness is sufficiently large for the absorption signal to build (for very thin clouds almost no absorption occurs, hence the SWIR/VIS ratio stays close to unity for both ice and liquid clouds), and (iii) the surface albedo in the SWIR band relative to the visible isn't too different.

With these considerations, the ratio of SWIR/VIS reflectances can provide useful information on the cloud thermodynamic phase when the optical thickness is greater than about 1 (King et al., 2004). As illustrated in the following section, an obvious limitation of this metric is that separation between ice and liquid phase can be ambiguous when the particle size becomes too large for liquid clouds or too small for ice clouds. However, this technique is not subject to cloud temperature bias nor systematic geometrical sampling effects except for the sunglint region over ocean.

---

angle polarisation measurements. Overview of an improved algorithm for POLDER3/PARASOL mission. submitted to IEEE Trans. Geo. and Remote Sensing, 2007.

EGU

2.3 Use of thermal infrared measurements

The bispectral technique discussed in Baum et al. (2003) and Platnick et al. (2003) is currently used for routine analysis of MODIS data. It is based on the fact that the imaginary part of the refractive index for ice and liquid are almost equal at 8.5 μm but diverge significantly around 11 μm with ice having greater absorption. The use of differential absorption properties is similar to the previous SWIR/VIS technique but infrared channels are used, making the inference of cloud phase independent of solar illumination. With this method, cloud analyses will be consistent between daytime and nighttime conditions.

Radiative transfer simulations indicate that the brightness temperature difference between the 8.5 and 11 μm bands (hereafter denoted as BTD[8.5–11]) tends to be positive in sign for ice clouds that have a visible optical thickness greater than approximately 0.5. Water clouds of relatively high optical thickness tend to exhibit negative BTD[8.5–11] values of generally less than -2 K.

In addition to the differences caused by the divergence in the refractive index for ice and water, the BTD[8.5–11] values are quite sensitive to atmospheric absorption, especially by water vapor. Also, these IR window bands are sensitive to the surface emittance properties. Recent studies have shown that the 8.5-μm surface emittance can decrease much more significantly than that at 11-μm over non-vegetated land. Thus, clear-sky BTD[8.5–11] values tend to be negative because of the difference in surface emissivity over non-vegetated surfaces between the two bands as well as from differing sensitivities to water vapor absorption. The BTD[8.5–11] value for low-level water clouds tends to become more negative as the water vapor loading increases and as particle size increases. Additionaly, small particles tend to increase the BTD[8.5–11] values relative to large particles because of increased scattering (assuming total ice water content is kept constant).

In summary this technique is subject to surface emissivity, water vapor, and to a lesser extent particle size biases but has the major advantage of being applicable

EGU

to both daytime and nightime measurements. There are known issues with this approach, primarily for optically thin cirrus, multilayer cloud systems in which optically thin cirrus overlies a low-level water cloud, and a single-layer cloud at temperatures between 238 K and 273 K. In this temperature range, one could make a case on the basis of radiative transfer simulations that either water or ice particles could be present (or a mixture of the two), so that one cannot make an unambiguous assessment of the phase. This is important because single-layered clouds of wide spatial extent having cloud-top temperatures in the range between 238 K and 270 K are prevalent in the storm tracks in both the Northern and Southern Hemispheres. While there are limitations, the MODIS bispectral IR algorithm reports an unambiguous cloud phase determination in approximately 80% of global data.

The MODIS operational algorithm provides two sets of information for cloud phase. One product is provided day and night at 5-km resolution and is based solely on the bispectral thermal infrared technique. The other product, used in the optical properties retrieval, is provided at 1-km resolution during the daytime only and is based on a combination of both SWIR, thermal IR, and additional information from individual cloud mask tests.

3 Algorithm description

3.1 Data fusion

The rationale for merging the three methods previously described is twofold. First, because each method has its own limitations, it is not always possible to provide a definitive phase determination based on a single technique. By implementing multiple approaches, the phase information content can be improved.

The second reason is that when all three methods provide a "reliable" answer, a general agreement between them provides a higher confidence level in the retrieval.

When they disagree, this information is again useful because it provides guidance for focused attention and potential for identification of multilayer situations or mixed phase clouds.

3.2 Implementation

In the first step, the algorithm is designed to compute a cloud phase index for each individual method and assign to each pixel one of the following: confident liquid, liquid, mixed, ice, confident ice or unknown (Fig. 4).

In our implementation, the polarization (POLDER) and bispectral thermal IR (MODIS) algorithms are obtained directly from application of a copy of the most recent production code software. However, we allow for more undetermined cases in the POLDER algorithm output when the decision is known to be less reliable (e.g., for poor observation geometries). Additionally, the cloud top pressure sanity check is not performed. Further details are provided in the Algorithm Theoretical Basis Documents for each method and their associated publications (Platnick et al., 2003, Riedi et al.[2]).

The SWIR/VIS method does not reproduce the more complex algorithm used in the MODIS optical properties phase product Platnick et al. (2003) (In MOD06 Collection 5 product: refer to Science Data Set *Cloud_Phase_Optical_Properties*). Only SWIR/VIS thresholds are applied (2.1 μm to 0.670 μm ratio over land; 2.1 μm to 0.865 μm ratio over ocean) and are given thresholds that provide an unambiguous decision of either ice or liquid phase. Such an implementation of the SWIR/VIS phase algorithm alone would yield a large proportion of undetermined cases if it was to be applied as a standalone phase retrieval scheme. This is counterbalanced here by the combination of the three methods.

In the subsequent step, the final decision is from these three individual indices based on a decision tree built from a priori expert knowledge that accounts for the potential strengths and weaknesses of each method. The decision tree starts by looking at the thermal IR phase index for which high confidence is not allowed. The main reasons for this are that (i) the algorithm can be applied everywhere with a minimum amount

EGU

of undetermined cases and (ii) it can be applied regardless of solar illumination. The use of this infrared method as a basis for the decision logic has the advantage of providing a maximum coverage of the final phase product and is expected to provide better day/night coherence.

Then, for each possible output of the thermal IR method (liquid, mixed, ice, unknown) the two other indices (SWIR/VIS and polarization) are compared and a decision is made depending on whether the two indices are in agreement with each other, and also whether they agree with the thermal IR test. The confidence level of each individual index is also considered for the final decision. Each possible combination is thus evaluated and accorded a value ranging from 0 (pure high confidence liquid) to 200 (pure high confidence ice). The highest confidence value is reached when all three indices agree with each other and are all at the highest possible confidence level for the class considered (the term class refers here to either the liquid, mixed or ice category).

For example, if two indices indicate liquid and the third index is ice, the final decision would be liquid but with a low confidence value (about 70). When one or two tests can not provide useful information, the remaining test will be used alone to take a decision and will always be accorded a low confidence value. The mixed phase situations tend to be denoted by a final index value around 100 and correspond to cases in which the individual tests do not agree with each other. Note that the final decision is not strictly a linear average of the three intermediate results as each combination has been evaluated invidually. Hence, a combination of 2 liquid and 1 ice intermediate results will not always provide the same final decision depending on which methods yielded the ice answer for instance. A typical mixed phase case situation would be for instance, a thermal IR index of mixed, a SWIR indicating ice and a polarization index indicating liquid. Hence, there is a difference in the final product between low confidence ice or water and mixed phase although the final index over an image has an almost continuous range of values from pure liquid to pure ice.

EGU

4 Theoretical performance consideration

Before discussing the case study, we discuss a number of theoretical scenarios to understand how the algorithm performs in particular situations.

4.1 Thin cirrus alone

5 The inference of phase for optically thin ice clouds (i.e., cirrus) can be problematic because both surface spectral properties and emissivity can bias the SWIR and thermal IR methods.

For the SWIR test, the thresholds have values such that in case of thin clouds, the ratio could be in the undetermined range. One exception is in the sunglint region over
10 ocean where the ratio can be high enough to lead to liquid phase. Over ocean in the sunglint region of MODIS, we use the POLDER data to evaluate the "out of glint" cloud reflectance. If the minimum reflectance at 0.865 μm observed by POLDER out of the glint region is lower than 0.1, the SWIR test is switched off to prevent false detection of liquid phase.

15 The thermal IR test is very sensitive to thin cirrus due to the strong signal of the BTD[8.5–11]. However, when the cirrus optical thickness is less than approximately 0.5 over oceans and warm, vegetated surfaces (where the surface emissivity is high in both IR bands), a false inference of liquid phase can occur (Baum et al., 2003). The misinterpretation of phase can occur at slightly higher values of cirrus optical thick-
20 nesses over non-vegetated surfaces such as deserts.

Fortunately, the problem is reversed for polarization measurements since clear skies yield a similar angular signature to ice clouds or very broken low liquid clouds. Hence, by default the polarization will tend to identify correctly thin cirrus clouds as ice clouds.

Overall, the thin cirrus may be partially misclassified as liquid by the SWIR and IR
25 tests but the polarization tests will reduce this bias or at least lower the confidence in the retrieval.

4.2 Thick ice/liquid clouds

For optically thick clouds, the SWIR/VIS signal is insensitive to surface spectral properties but the potential particle size bias remains. The SWIR reflectance will saturate more rapidly than the VIS reflectance as cloud optical thickness increases. Subsequently, the SWIR/VIS ratio will decrease accordingly for both ice and liquid clouds and for all particle effective sizes.

Consequently, the probability that the SWIR/VIS ratio for liquid clouds decreases below some given threshold will increase as cloud optical thickness increases. This tendency occurs regardless of particle size. In this asymptotic regime, we can determine from theoretical values of the SWIR and VIS reflectances (computed for different values of effective radius and optical thickness), that there exists an extended range of (τ_c, R_{eff}) combinations where ice and liquid phase clouds are indistinguishable using a simple SWIR/VIS ratio. Figure 3 illustrates the overlap between ice and liquid phase solution spaces in a 2.1–0.865 μm reflectance diagram.

The situations may not be as dramatic as it appears in Fig. 3 because as liquid cloud optical thickness increases, the probability of having larger droplets increases (not that the reverse isn't necessarily true for ice clouds). It remains that the SWIR/VIS ratio metric will provide unambiguous information only for liquid clouds with R_{eff} less than 8.0 microns or ice clouds with R_{eff} greater than 30 microns.

As can be seen from inspection of Fig. 4, this implies that the potential exists for numerous pixels to remain unclassified using the SWIR/VIS metric. For all these cases, the additional information from the IR bispectral and polarization techniques will be necessary to provide reliable phase determination.

The BTD[8.5–11] signal is affected by smaller particle sizes because of the increased scattering, but the information provided becomes ambiguous in case of supercooled liquid clouds when cloud top temperature is in the 238 K–270 K range. As with the SWIR test, one could make a case for either water or ice in this range based on a range of simulated conditions. A significant number of undetermined or mixed cases for these

clouds would benefit from additional information from SWIR/VIS and polarization tests.

Note finally that for optically thick clouds, the polarization signal is strong and unambiguous as long as cloud cover is not broken and the angular range available is sufficient. The main limitation remaining is that polarization provide information for the very top of the cloud, or into the cloud up to an optical thickness of 3.

4.3 Thin ice cloud over liquid

Multilayered clouds, and in particular the case where an ice cloud overlies a lower-level liquid cloud, are problematic for any passive retrieval of cloud properties because for practical purposes, current operational algorithms have to assume a single-layered cloud of homogeneous phase. For multilayered clouds, a single phase obviously cannot represent the situation. As a consequence, an obvious problem occurs when a cloud optical property model has to be chosen from a static look-up table for the subsequent retrieval of optical thickness and particle effective size.

To improve the situation, the first step would be to detect when multilayered clouds occur. This is the subject of some recent work (Pavolonis and Heidinger, 2004; Pavolonis et al., 2005). In the case of relatively thin cirrus, the different sensitivities of the three phase discrimination methods can provide useful information depending on the cirrus optical thickness.

To evaluate our ability to detect a multilayered cloud situation, we have simulated the different metrics used in our algorithm for an ice cloud of varying optical thickness (between 0 and 10) overlying a lower-level liquid cloud layer of constant optical thickness (10). Figures 5, 6, 7 and 8 present respectively the simulated metrics used for polarization, shortwave infrared and thermal infrared based retrievals.

For SWIR/VIS and IR simulations, the ice crystal model is a perfect hexagonal column of aspect ratio 1 with a spherical equivalent volume of 40 μm. We choose a simple model for which all optical properties can be easily and coherently computed for the various wavelengths involved in our retrievals. For polarization simulations, we used the IHM model from Labonnote et al. (2001) which proved to best match the polarized

angular signature of ice clouds on a global scale (Baran and Labonnote, 2006). The liquid cloud model is a gamma size distribution of spheres with an effective radius of 12 μm and an effective variance of 0.1.

An adding-doubling code was used to compute polarized reflectances De Haan et al. (1987) whereas an accurate Fast Discrete Ordinate Method (Dubuisson et al., 1996; Dubuisson et al., 2005), which accounts for absorption and scattering, has been used for cloud radiance computations in all visible, shortwave infrared and thermal infrared bands.

Polarized reflectances tend to saturate for optical thicknesses greater than 2. For cirrus optical thicknesses less than 2, the liquid cloud signature is still present in the polarized reflectances in the rainbow scattering angle region (around 140°) as can be seen from Fig. 5.

For a cirrus optical thickness less than 1, the polarization signature will be classified as "liquid" by the POLDER standalone algorithm. Between 1 and 2, the polarization signature will be interpreted as a "mixed" or "undetermined" case; an optical thickness greater than 2 will yield "ice" phase. If the rainbow region is not sampled by the measurements, the "mixed" case can not be identified.

The situation is more complex with the SWIR/VIS metric since the respective contribution from absorption and scattering will build up differently depending on the particle size of both the liquid and ice clouds. However, we can still evaluate approximate upper and lower limits of this metric by looking at an asymptotic regime of this ratio. Simulations are performed for two solar geometries (nadir and 30°), 10 view zenith and 20 relative azimuth geometries.

On Figs. 6a and 6b, the SWIR/VIS theoretical ratios are plotted for each cirrus optical thickness, as a function of viewing angle by averaging over relative azimuth angle. This was done to provide a crude estimate for the magnitude of variation one could expect from a set of realistic cloud conditions. If we consider the average ratio for pure liquid cloud (0.75 for cirrus optical thickness = 0.) and allow a 0.1 (0.2) variation from this initial value, then we can see that when thin cirrus OT is less than 0.2 (0.5), the phase

Cloud phase from POLDER and MODIS data

J. Riedi et al.

Title Page

Abstract	Introduction
Conclusions	References
Tables	Figures

◀◀	▶▶
◀	▶
Back	Close

Full Screen / Esc

Printer-friendly Version

Interactive Discussion

EGU

will be returned as liquid. Conversely, considering the thick ice cloud limit (0.15) and allowing an equivalent 0.1 (0.2) increase for the ratio would lead to a limit of cirrus OT of about 3.0 (2.0) above which a single-layered ice cloud can not be distinguished from a multilayered cloud scenario.

Another way to consider the problem is to consider the thresholds used for intermediate phase retrieval based on SWIR/VIS ratio. The thresholds have been set experimentally and result partially from the analysis of a large number of MODIS scenes during the validation and quality assessment phase of MODIS cloud optical properties collection 5 products. The PDF of the ratio values is divided into 5 regions using thresholds at 0.65, 0.55, 0.35 and 0.25, which correspond respectively to confident liquid, probably liquid, unknown, probably ice, and confident ice. These thresholds are demonstrated in Figs. 6c and 6d, where the SWIR/VIS theoretical ratios are plotted on a surface as a function of both cirrus OT and viewing geometry. It can be seen from this that confident liquid (ice) will be assessed only if the overlaying cirrus OT is lower (greater) than 0.2 (3.0).

The reduced confidence thresholds occur respectively for liquid and ice at cirrus optical thicknesses of about 0.5 and 2. With this single criterion, a multilayered cloud situation consisting of ice over water clouds, in which the cirrus optical thickness lies between 0.5 and 3, will most probably lead to a low confidence or undetermined phase. Note that these threshold values, derived from statistical analysis of real observations, are consistent with those derived by allowing a 0.1 departure from pure liquid or ice theoretical ratio values. An important observation also is that this metric seems to present very limited dependance on viewing or solar geometries, which justify the applicability of fixed thresholds with respect to the observation geometry, and in consideration of other uncertainties linked to particle size, for example.

When the $11\,\mu m$ brightness temperature is in the range of $238\,K$ to $268\,K$ where ice and supercooled liquid water can coexist, the bispectral IR algorithm is basically selecting the phase based on BTD[8.5–11] values using a set of thresholds at 0.5, -0.25 and $-1.0\,K$, delimiting the regions of Ice, Unknown, Mixed and Liquid.

Figures 7 and 8 illustrate the sensitivity of BTD[8.5–11] to cirrus optical thickness and to atmospheric profile. Brightness temperatures at 8.5 and 11 μm depend strongly on each cloud layer altitude (temperature), particle size, water vapor profile, and surface emissivity. It is difficult to evaluate all possible combinations of atmospheric profile, cirrus altitude and optical thickness, and liquid cloud altitude. We have chosen to illustrate only a few problems using simulations performed with four distinct scenarios.

Two cases are considered in which the liquid cloud layer is located at either 5 km (Fig. 7) or 2 km (Fig. 8), with the cirrus cloud being kept at 10 km. For each case, two very different atmospheric profiles are considered (MidLatitude Summer, humid and warm; SubArctic Winter, dry and cold). Finally, the thresholds used for the IR phase retrieval are indicated on each of the BTD[8.5–11] figures.

A first observation is that the location of the lower liquid cloud has a moderate influence on the observed BTD[8.5–11], but this influence is more pronounced (as expected) for the warm/humid profile. For the MidLatitude Summer profile, the cirrus temperature is set at about 248 K. From the corresponding BTD[8.5–11] diagrams on Fig. 7 and 8, it seems that all situations will be declared Liquid for cirrus OT up to about 2.0 and will then be declared Mixed or Unknown depending on the value of the cirrus OT. This clearly illustrates the potential bias in the IR retrieval in the case of multilayered clouds in a warm/humid atmosphere. For the SubArctic Winter profile, and again for both liquid cloud altitudes, the phase will rarely be declared as Liquid since the BTD[8.5–11] value increases above the −1.0 threshold for cirrus optical thickness as low as 0.1 or 0.2 depending on the viewing geometry. The phase may be declared as Mixed for cirrus OT up to 0.5 and will be Unknown until the cirrus optical thickness reaches a value of 2 unless the 11 μm BT passes below the 238 K threshold.

For additional discussion about the sensitivity of BT11 and BTD[8.5–11] we suggest reading, among others, the studies from Baum et al. (2000), Strabala et al. (1994) and Baum et al. (2003).

This sensitivity study is obviously limited but clearly illustrates again the difficulty of dealing with supercooled and/or multilayer clouds. However, we have shown that the

polarization, SWIR/VIS and TIR metrics will behave quite differently in these situations, providing potential information to identify multilayer situations as shown by Nasiri et al. (2004) using MODIS data only. The identification of multilayer situations in case of Mixed phase (as determined by our multisensors algorithm) will be done a posteriori

5 by combining the phase index with other information such as different cloud pressure retrievals or observations from active sensors.

4.4 Mixed phase

Mixed phase clouds are obviously problematic and therefore of primary interest for our current investigation. When liquid spherical droplets coexist with ice particles, we

10 anticipate that high absorption by ice will show up in the SWIR band and also that BTD[8.5–11] may indicate either mixed or undetermined phase.

However, spherical particles can produce a rainbow feature that will toggle a liquid phase detection in the polarization test. Opposing decisions from the SWIR/VIS and polarization tests, with mixed or undetermined phase from IR test, will lead to confident

15 mixed phase in the final index.

Again, additional information to discriminate multilayer clouds from single layer mixed-phase clouds will then be needed to decide whether mixed phase is due to vertical structure or inherent to the single cloud layer. Work is under progress to use different pressure retrievals from POLDER and MODIS to help detect the presence of

20 multilayer clouds. Also, the multilayer flag product available from MODIS MYD06 cloud product can provide some information and is under investigation, being a new product. Both will obviously require validation from the active lidar in the A-Train.

Table 1 summarizes the basic principles and potential biases for each of the three methods used to develop the joint algorithm.

Cloud phase from POLDER and MODIS data

J. Riedi et al.

Title Page

Abstract	Introduction
Conclusions	References
Tables	Figures

◄◄   ►►

◄   ►

Back   Close

Full Screen / Esc

Printer-friendly Version

Interactive Discussion

EGU

5 Case study analysis and discussion

The case study selected to illustrate the present approach includes Typhoon Nabi on 2 September 2005. This portion of a PARASOL orbit was selected due to the presence of a typhoon over ocean and a large cloud system over land. Both scenes contain both optically thin and thick clouds at different levels, thus providing an a priori complex case for which individual phase retrieval methods might provide ambiguous information.

We discuss hereafter particular cloud situations available from this case study. For each, results for individual phase discrimination tests are discussed, as well as how each test contributes to the final decision. The final decision takes into account the limitations and advantages of each method.

5.1 Northern Scene

The cloud system in the northern part of Fig. 1 provides a very good example of a midlevel cloud layer (see Oxygen cloud pressure retrieval on Fig.9b). Most of these clouds have temperatures between 238 K and 268 K where ice and supercooled liquid water can coexist. Figure 4 shows that a significant portion of the cloud system indicates an ambiguous signal for the SWIR/VIS metric that is thought to be associated with large liquid particles since both polarization and TIR tests agree on Liquid phase. The ice cloud part of the cloud system is retrieved fairly coherently in all three methods leading to high confidence ice in the final retrieval shown in Fig. (9a).

Finally, the pixels declared as Mixed phase by the TIR method are given a lower confidence Liquid flag in the polarization test and the Unknown flag from the SWIR/VIS test. As can be seen from the O2 pressure retrieval, those Mixed phase pixels have a slightly higher altitude than some surrounding high confidence Ice pixels, perhaps indicating a multilayer cloud situation. This will be further evaluated using active sensors in future work.

EGU

5.2 Typhoon Scene

Investigation of a portion of Typhoon Nabi in the southern part of Fig. 1 provides further insight as to how the three methods can provide a very different perspective of a given situation.

⁵ The top of the typhoon is located very high in the atmosphere and whether it is optically thick or not does not make much difference in the TIR retrieval, indicating a large extent of the cirrus cloud layer (Fig. 9a). The situation is more ambiguous again with the SWIR/VIS metric (Fig. 9b), which turns rapidly from confident Ice about the center of Nabi to Unknown without seeing very many lower confidence Ice pixels.

¹⁰ Finally the polarization test (Fig. 4a) indicates clearly the presence of liquid cloud layer just north of Nabi's eye and also in the western and south-western region of the typhoon. For these pixels, the final cloud phase index range from low confidence Ice to high confidence Mixed. It is evident from inspection of individual metrics on Fig. 2 and O2 cloud pressure on Fig. 9b that most of these pixels correspond to multilayer clouds

¹⁵ where high thin cirrus overlays a lower-level liquid cloud layer. Note also that the partial phase indices (Fig. 4) are very consistent in this particular case with what has been discussed in the theoretical part related to performance of the algoritm in case of thin cirrus over low water clouds. Again, these findings would need to be validated using active sensor observations available from CALIPSO and CloudSat in the A-Train. How-

²⁰ ever, this is beyond the scope of the present paper which aims primarily at describing the theoretical basis and implementation of our synergistic algorithm.

5.3 Final phase index

Figure 9a presents the final results of our joint POLDER/MODIS algorithm together with the cloud pressure derived from Oxygen A-Band (Fig. 9b). At this stage, we can

²⁵ comment on two facts. First, the cloud phase index presents fairly smooth variation indicating that the logical decision tree does not yield unstable situations where we would randomly switch between confident ice and confident liquid. Secondly, the phase index

EGU

behaves fairly coherently compared to cloud O2 pressure even if this information is not involved in the phase retrieval process. Overall, and before a thorough validation is performed using active sensors, we conclude from this case study (and others, not shown/discussed here) that our proposed method provides new and relevant information on cloud thermodynamic phase and to a lesser extent on the vertical structure of cloud layers.

6 Conclusions

With the use of coincident data available from POLDER3/Parasol and MODIS/Aqua, three independent methods for deriving cloud phase have been applied singly and in combination. It is shown that these methods can provide different information for a single-layered cloud due to their respective sensitivity to different parameters. For unambiguous cases where all three methods provide the same answer individually, the combination is still useful since it can be used to assess the confidence level of the phase retrieval. For cases where the three methods disagree, an attempt is made to interpret the differences in terms of multilayer clouds and/or single-layered mixed phase clouds.

Validation of the retrieved joint product is outside the scope of this paper but we can expect the combination of well evaluated methods to provide at least an equally accurate product. The value added by the synergy of POLDER and MODIS relies mainly in (i) the confidence index associated with the product, (ii) the potential to clearly identify mixed phase cases and (iii) to a lesser extent, the possibility of determining an index for almost every pixel that uses the strengths of each method.

In future research, a thorough analysis of the full joint dataset provided by POLDER3/Parasol and MODIS/Aqua will provide statistics of this new product. Obviously, with the availability of CloudSat and CALIPSO, it is expected that a large validation dataset containing vertical profile information will help us in evaluating the statistical meaningfulness of each class of the decision look-up table. However, a cloud

phase product from CALIOP (the depolarization lidar on the CALIPSO platform) is not currently available but is slated for release in the near future.

If a reasonable correlation between radar/lidar data and the phase index can be demonstrated in case of multilayer or mixed phase clouds, the POLDER/MODIS combination will prove extremely useful to extend the vertical information from the active instruments to the full swath covered by the passive instruments of the A-Train.

References

Baran, A. J. and Labonnote, L. C.: On the reflection and polarization properties of ice cloud, J. Quant. Spect. Rad. Transfer., 100, 41–54, 2006. 14117

Baum, B. A, Soulen, P. F., Strabala, K. I., King, M. D., Ackerman, S. A., Menzel, W. P., and P. Yang: Remote sensing of cloud properties using MODIS airborne simulator imagery during SUCCESS: 2. Cloud thermodynamic phase, J. Geophys. Res, 105, 11 781–11 792, 2000. 14105, 14119

Baum, B. A., Frey, R. A., Mace, G. G., Harkey, M. K., and Yang, P.: Nighttime multilayered cloud detection using MODIS and ARM data, J. Appl. Meteorol., 42, 905–919, 2003. 14105, 14110, 14114, 14119

Bréon, F. M. and Goloub, P.: Cloud droplet effective radius from spaceborne polarization measurements, Geophys. Res. Lett., 25, 1879–1882, 1998. 14108

Chepfer H., Goloub, P., Riedi, J., De Haan, J. F., Hovenier, J. W., and Flamant, P. H.: Ice crystal shapes in cirrus clouds derived from POLDER-1/ADEOS-1., J. Geophys. Res., 106, 7955–7966, 2001. 14108

De Haan, J. F., Bosma, P. B., and Hovenier, J. W.: The adding method for multiple scattering calculations of polarized light, Astron. Astrophys., 183, 371–391, 1987. 14117

Dubuisson P., Buriez, J.-C., and Fouquart, Y.: High spectral resolution solar radiative transfer in

Cloud phase from POLDER and MODIS data

J. Riedi et al.

EGU

absorbing and scattering media application to the Satellite Simulation, J. Quant. Spect. and Rad. Transfer., 55, 103–126, 1996. 14117

Dubuisson P., Giraud, V., Chomette, O., Chepfer, H., and Pelon, J.: Fast radiative transfer modeling for infrared imaging radiometry, J. Quant. Spect. and Rad. Transfer., 95, 201–220, 2005. 14117

Goloub, P., Herman, M., Chepfer, H., Riedi, J., Brogniez, G., Couvert, P. and Séze, G: Cloud Thermodynamical Phase Classification from the POLDER Spaceborne instrument, J. Geophy. Res., 105, 14 747–14 759, 2000. 14105, 14106, 14108

Hahn, C. J., Warren, S. G., London, J., Chervin, R. M., and Jenne, R.: Atlas of simultaneous occurrence of different cloud types over the ocean, NCAR Tech. Note TN-201 STR, 212 pp, 1982 14105

Hahn, C. J., Warren, S. G., London, J., Chervin, R. M., and Jenne, R.: Atlas of simultaneous occurrence of different cloud types over land. NCAR Tech. Note TN-241 STR, 209 pp, 1984. 14105

Hutchison, K. D., Etherton, B. J., Topping, P. C., and Huang, H. L.: Cloud top phase determination from the fusion of signatures in daytime AVHRR imagery and HIRS data, Int. J. Remote Sensing, 18, 3245–3262, 1997.

Key, J. and Intrieri, J.: Cloud particle phase determination with the AVHRR, J. Appl. Meteorol., 39, 1797–1805, 2000. 14105

King, M. D., Platnick, S., Yang, P., Arnold, G. T., Gray, M. A., Riedi, J. C., Ackerman, S. A., and Liou, K. N.: Remote sensing of liquid water and ice cloud optical thickness, and effective radius in the arctic: Application of airborne multispectral MAS data, J. Atmos. Ocean. Tech., 21, 857–875, 2004. 14109

Knap, W., Stammes, P., and Koelemeijer, R. B. A.: Cloud thermodynamic phase determination from near-infrared spectra of reflected sunlight, J. Atmos. Sci., 59, 83–96, 2002. 14105

Labonnote, C.-L., Brogniez, G., Buriez, J. C., Doutriaux-Boucher, M., Gayet, J. F., and Macke, A.: Polarized light scattering by inhomogeneous hexagonal monocrystals, Validation with ADEOS-POLDER measurements, J. Geophy. Res., 106, 12 139–12 153, 2001. 14116

Lee, J., Yang, P., Dessler, A. E.,Baum, B. A., and Platnick,,S.: The influence of thermodynamic phase on the retrieval of mixed-phase cloud microphysical and optical properties in the visible and near-infrared region, IEEE, Geosci. Remote Sens. Lett., 3, 287–291, 2006.

Moody, E. G., King, M. D., Platnick, S., Schaaf, C. B., and Gao, F.: Spatially complete global spectral surface albedos: Value-added datasets derived from Terra MODIS land products,

Title Page

Abstract | Introduction

Conclusions | References

Tables | Figures

◄ | ►│

◄ | ►

Back | Close

Full Screen / Esc

Printer-friendly Version

Interactive Discussion

EGU

IEEE, Trans. Geosci. Remote Sens., 43, 144–158, 2005. 14106

Nasiri, S. L. and Baum, B. A.: Daytime multilayered cloud detection using multispectral imager data, J. Atmos. Ocean. Tech., 21, 1145–1155, 2004. 14120

Parol, F., Buriez, J., Brogniez, G., and Fouquart, Y.: Information Content of AVHRR Channels 4 and 5 with Respect to the Effective Radius of Cirrus Cloud Particles, J. Appl. Meteorol., 30, 973–984, 1991.

Parol, P., Buriez, J. C., Vanbauce, C., Riedi, J., Labonnote, L. C., Doutriaux-Boucher, M., Vesperini, M., Séze, G., Couvert, P., Viollier, M., Bréon, F. M.: Capabilities of multi-angle polarization cloud measurements from satellite: POLDER results, Adv. Space Res., 33, 1080–1088, 2004. 14106

Pavolonis, M. J. and Heidinger, A. K.: Daytime cloud overlap detection from AVHRR and VIIRS, J. Appl. Meteorol., 43, 762–778, 2004. 14105, 14116

Pavolonis, M. J., Heidinger, A. K., and Uttal, T.: Daytime global cloud typing from AVHRR and VIIRS: Algorithm description, validation, and comparisons, J. Appl. Meteorol., 44, 804–826, 2005. 14105, 14116

Pilewskie P. and Twomey, S.: Cloud phase discrimination by reflectance measurements near 1.6 and 2.2 μm, J. Atmos. Sci., 44, 3410–3420, 1987. 14109

Platnick S., King, M. D., Ackerman, S. A., Menzel, W. P., Baum, B. A., Riedi, J., and Frey, R. A.: The MODIS Cloud Products: Algorithms and Examples from Terra. IEEE, Trans. Geo. and Remote Sensing, 41, 459–473, 2003. 14105, 14106, 14110, 14112

Riedi J., Goloub, P., and Marchand, R. T.: Comparison of POLDER cloud phase retrievals to active remote sensors measurements at the ARM SGP site. Geophys. Res. Lett., 28–11, 2185–2188, 2001. 14106

Strabala, K. I., Ackerman, S. A., and Menzel, W. P.: Cloud Properties inferred from 8-12-μm Data, J. Appl. Meteorol., 33, 212–229, 1994. 14119

Takano, Y., Liou, K. N., and Minnis, P.: The Effects of Small Ice Crystals on Cirrus Infrared Radiative Properties, J. Atmos. Sci., 49, 1487–1493, 1992.

Tian, L. and Curry, J. A.: Cloud overlap statistics, J. Geophy. Res., 94, 9925–9935, 1989.

Vanbauce, C., Buriez, J. C., Parol, F., Bonnel, B., Séze, G., and Couvert, P.: Apparent pressure derived from ADEOS-POLDER observations in the oxygen A-band over ocean, Geophys. Res. Lett., 25, 3159–3162, 1998.

Vanbauce, C., Cadet, B., and Marchand, R. T.: Comparison of POLDER apparent and corrected oxygen pressure to ARM/MMCR cloud boundary pressures, Geophys. Res. Lett., 30,

Title Page

Abstract | Introduction

Conclusions | References

Tables | Figures

◄◄ | ►►

◄ | ►

Back | Close

Full Screen / Esc

Printer-friendly Version

Interactive Discussion

EGU

16.1–16.4, 2003.

Warren S. G., Hahn, C. J., and London, J.: Simultaneous occurrence of different cloud types, J. Climate Appl. Meteor., 24, 658–667, 1985.

Cloud phase from POLDER and MODIS data

J. Riedi et al.

Full Screen / Esc

Printer-friendly Version

Interactive Discussion

EGU

EGU

Table 1. Summary of methods main characteristics and limitations.

	Polar.	SWIR/VIS	Thermal IR
Sensitivity To Cloud Properties			
Particle shape	yes	no	no
Particle absorption	no	yes	yes
Particle size	no	yes	moderate
Potential Biases			
Obs. Geometry	yes	no	no
Temperature profile	no	no	yes
Water Vapor profile	no	no	yes
Particle Size	no	yes	moderate
Fractional Cloud Cover	yes	moderate	moderate
Surface albedo/emissivity	no	yes	yes
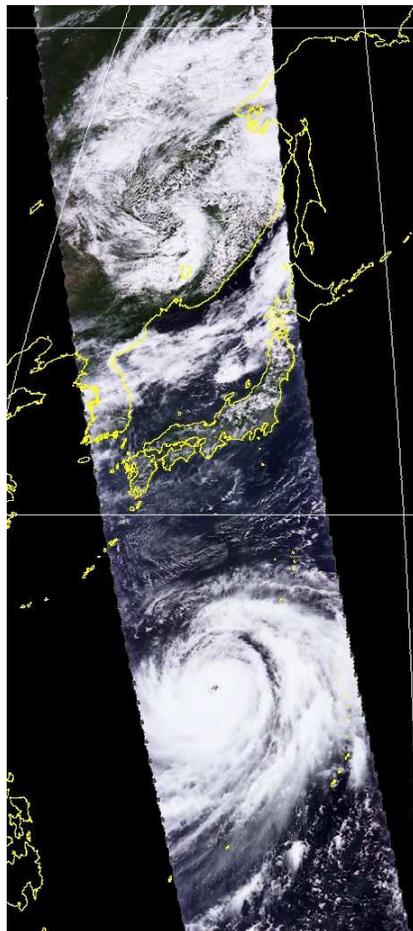
Fig. 1. POLDER true color composite of the common scene observed by MODIS and PARASOL on 2 September 2005 (MODIS swath is larger than POLDER). The southern part of the image is typhoon Nabi.

EGU
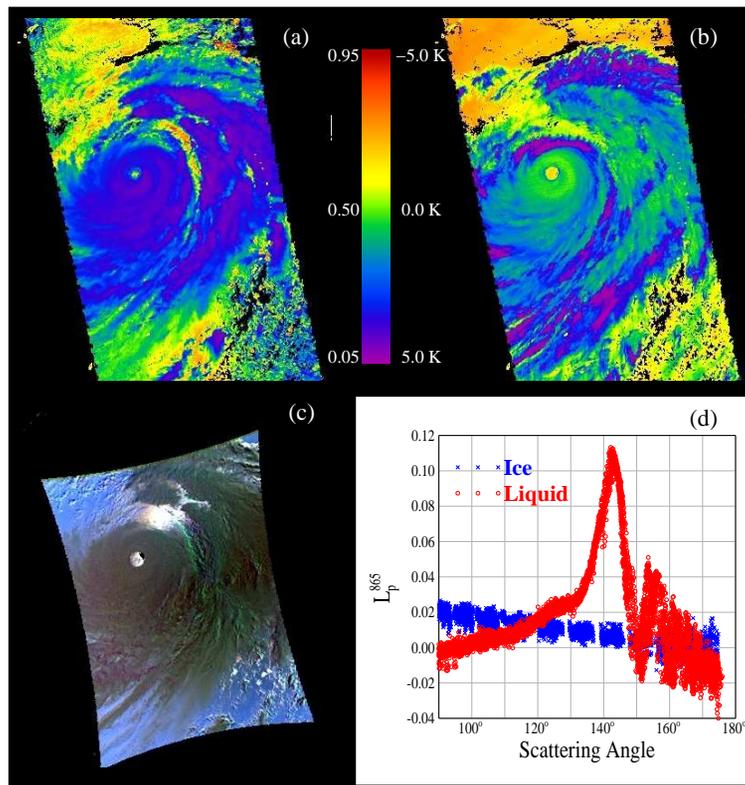
Fig. 2. Illustration over typhoon Nabi of the 3 metrics used for phase determination : **(a)** ratio of shortwave infrared to visible channel (2.1 to 0.865 microns), **(b)** brightness temperature difference between 8.5 and 11 microns channel, **(c)** false color composite from 490, 670 and 865 nm polarized reflectance for one instantaneous POLDER field of view, and **(d)** typical multi-angular polarized reflectance signature of liquid (red) and ice (blue) clouds.
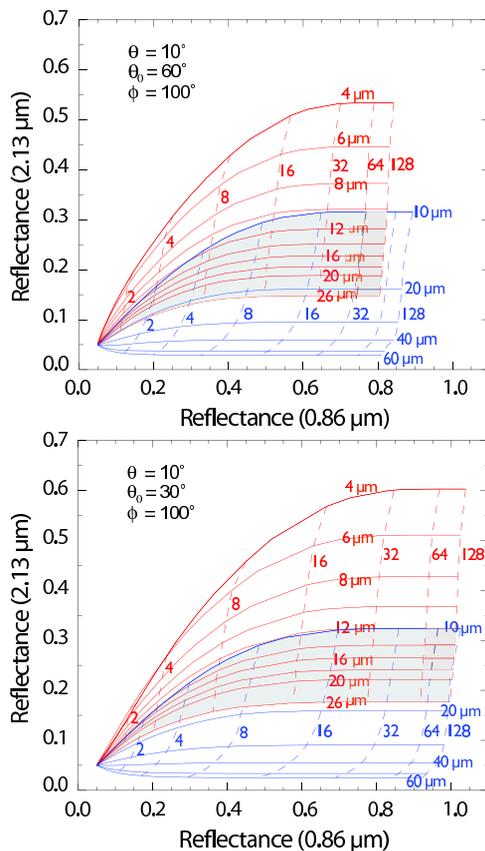
Fig. 3. Simulation for two solar geometries of the 2.1 μm against 865 nm reflectances for an ice (blue) and liquid (red) cloud of varying optical thickness and effective radius. Overlapping zone between the ice and liquid retrieval spaces (shaded region) corresponds to situation where SWIR/VIS metric can not provide unambiguous phase information.

Title Page

Abstract | Introduction

Conclusions | References

Tables | Figures

◄ | ►

◄ | ►

Back | Close

Full Screen / Esc

Printer-friendly Version

Interactive Discussion

EGU

EGU
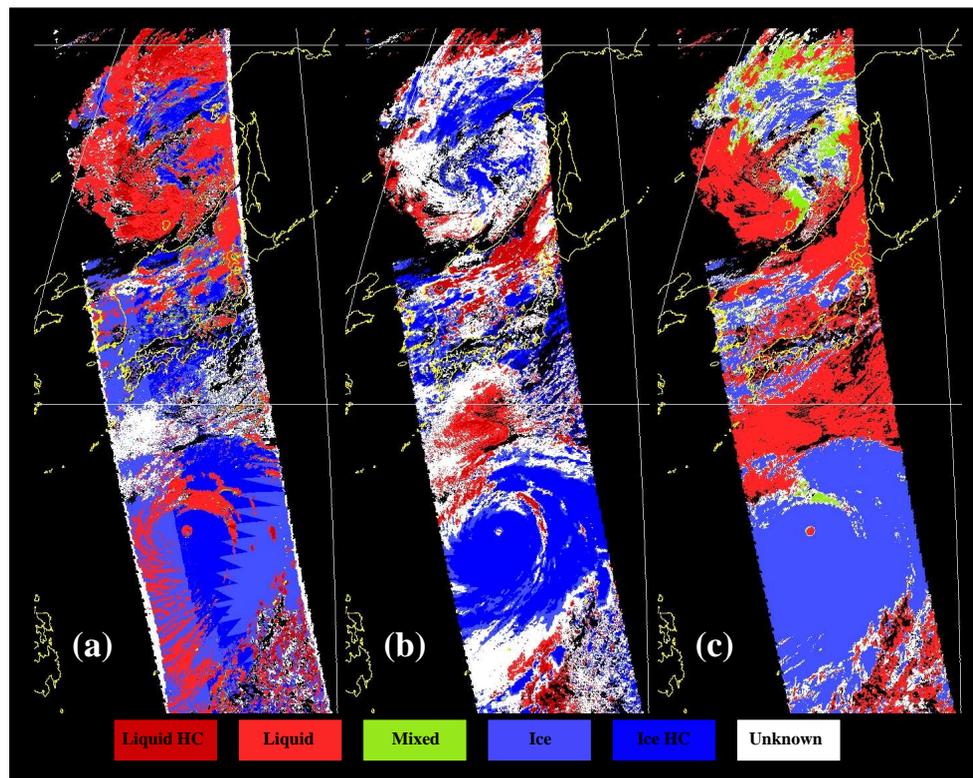
Fig. 4. Results of the partial cloud phase index retrieved from **(a)** POLDER polarization algorithm, **(b)** MODIS SWIR based algorithm and **(c)** MODIS bispectral IR algorithm.

Fig. 5. Simulation of polarized reflectance at 865 nm as a function of scattering angle for an ice cloud of varying optical thickness overlaying a lower liquid water cloud of optical thickness 10.
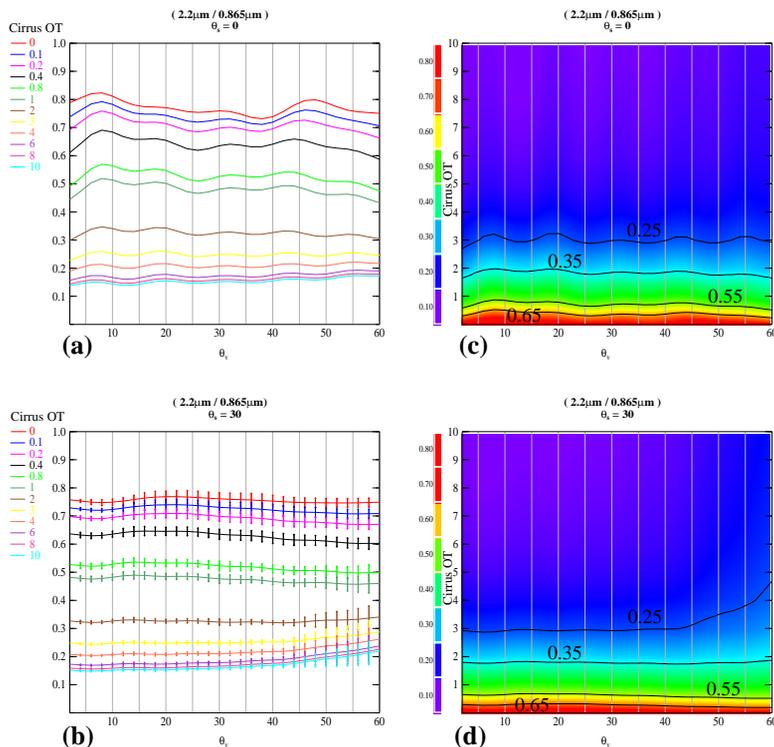
Fig. 6. Simulation for different geometries of the 2.1 μm to 865 nm reflectance ratio for an ice cloud of varying optical thickness overlaying a lower liquid water cloud of optical thickness 10. Panels **(a)** and **(b)** present the simulated ratio for different cirrus optical thickness as a function of viewing angle. Results are averaged over relative azimuth and standard deviations are indicated using error bars. Panels **(c)** and **(d)** present the same results as a surface contour of simulated ratio, function of viewing angle and cirrus optical thickness. The later representation is used to better illustrate the different regions defined by the SWIR/VIS thresholds used in our algorithm.

Title Page

Abstract | Introduction

Conclusions | References

Tables | Figures

◄ | ►

◄ | ►

Back | Close

Full Screen / Esc

Printer-friendly Version

Interactive Discussion

EGU
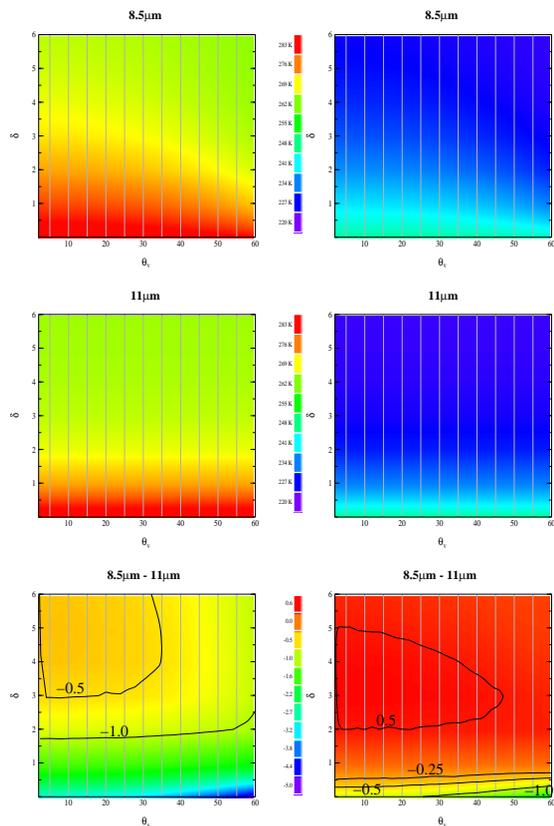
Fig. 7. Simulation for a Mid-Latitude Summer (left) and a Sub-Arctic Winter (right) atmospheric profile of the brightness temperature differences (in Kelvin) between channel at 8.5 and 11 μm as a function of view angle for an ice cloud of varying optical thickness at 10 km overlaying a lower liquid water cloud of optical thickness 10, located at 5 km. Isolines correspond to the thresholds used in the bispectral IR phase determination

Cloud phase from POLDER and MODIS data

J. Riedi et al.

Title Page

Abstract	Introduction
Conclusions	References
Tables	Figures

◄◄ ►►

◄ ►

Back Close

Full Screen / Esc

Printer-friendly Version

Interactive Discussion
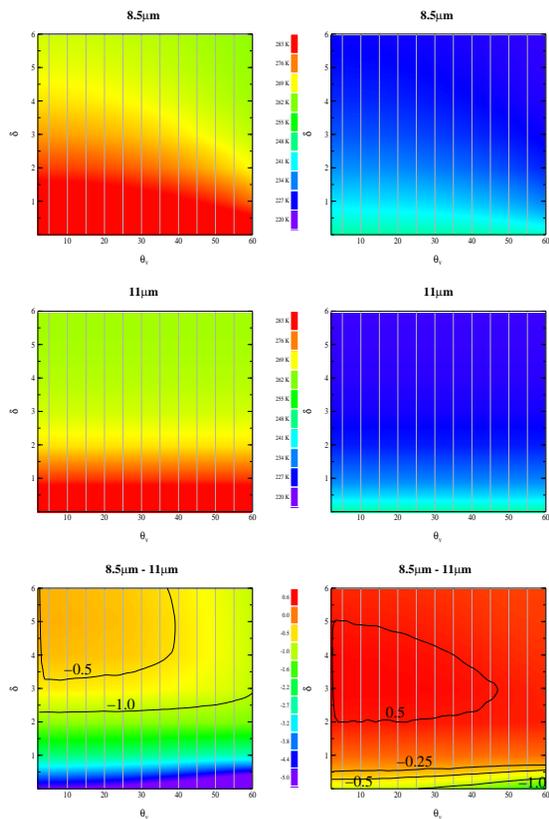
**Fig. 8.** Same as Fig. 8a but liquid cloud is located at 2 km.

EGU
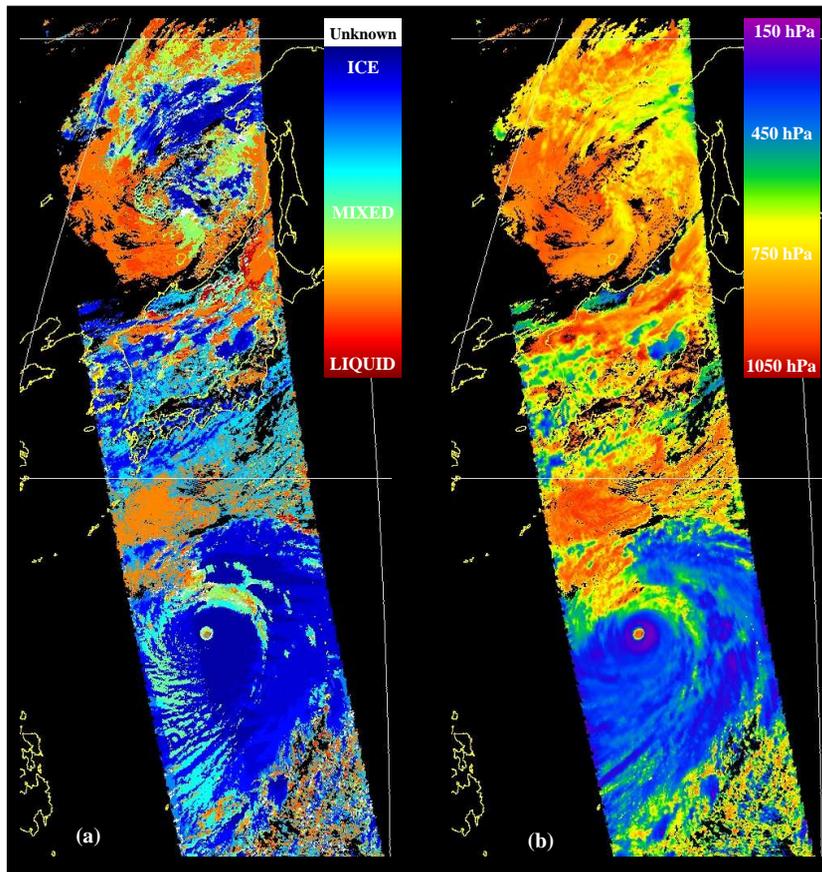
Fig. 9. (a) Results of the final cloud phase index retrieved from combination of POLDER and MODIS data. **(b)** Cloud top pressure derived from POLDER oxygen A-Band method.

Title Page

Abstract | Introduction

Conclusions | References

Tables | Figures

◄ | ►

◄ | ►

Back | Close

Full Screen / Esc

Printer-friendly Version

Interactive Discussion

EGU